XXI IMEKO World Congress "Measurement in Research and Industry"
August 30 – September 4, 2015, Prague, Czech Republic

# IMPEDANCE SPECTROSCOPY: SEPARATION AND ASYMPTOTIC MODEL INTERPRETATION

*Sioma Baltianski* [1]

[1] Wolfson Dept. of Chemical Engineering, Technion – Israel Institute of Technology, Haifa, Israel, cesema@technion.ac.il

***Abstract*** – A new and efficient technique of impedance spectra interpretation is presented. The decomposition of the full impedance into separate parts is accomplished by fitting data using a parametric distribution function of relaxation times in a convoluted form. Each particular impedance element is presented as the asymptotic model in the next step. The result of this procedure is unambiguous. This is demonstrated using electroceramic samples in the ranges $T$=200-475 ºC and $f$=10 mHz-30 MHz.

***Keywords***: Impedance spectroscopy, ambiguity, asymptotic model

## 1. INTRODUCTION

Impedance spectroscopy (IS) has attracted much attention as a non-destructive and effective analysis technique in many areas of materials science and device manufacturing.

Analysis, or the data interpretation of impedance spectroscopy, is not a straightforward task. In the simplest cases, an equivalent circuit with well-defined time constants can be found, while in more complex cases, the time constants are distributed. The major shortcoming of direct electrical model fitting is the ambiguity of the obtained results. A different approach to interpretation of impedance results is the construction of the so-called distribution function of relaxation times (DFRT). The data fitting is carried out using the convoluted form of DFRT.

Construction of the DFRT as the first step in our treatment allows an unambiguous separation of the complete distribution function of relaxation times into independent parametric segments that may be treated separately. The final step is the construction of an asymptotic model.

## 2. IMPEDANCE DATA SEPARATION

In some cases, the total impedance can be represented as independent sections, Fig. 1. Each of the partial impedances is a process or a constructive feature of the studied object.

The individual impedances can be represented as a cell (lumped elements) and a relaxation core (distributed part), Fig. 2.

In particular, we are interested in the cell parameters, the total capacity of the relaxation processes and its characteristic time constant.

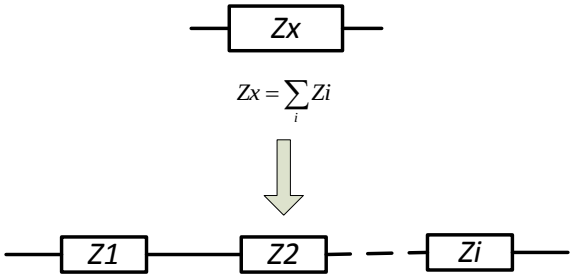


Fig. 1. Presentation of total impedance as a series of the partial impedances.

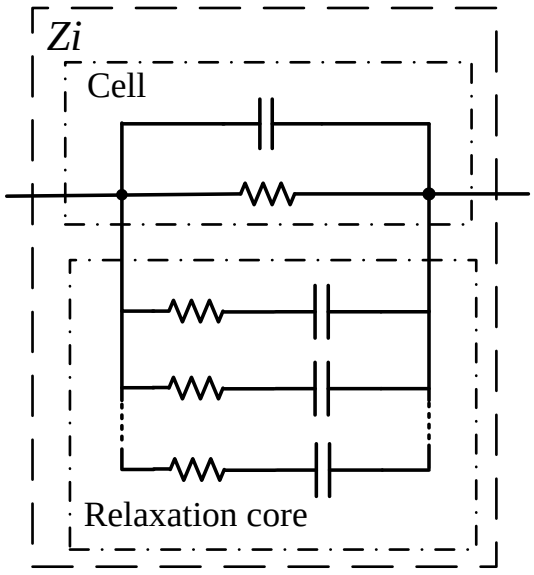


Fig. 2. Cell and relaxation core of the individual impedance *Zi*.

The most common approach for analyzing impedance spectroscopy, particular in electroceramics, is constructing an equivalent circuit. It is typically composed of *RC*-elements, with many variations on this theme. The direct fitting of the series-connected models, like in Fig. 2, will produce significantly different results if we change the initial parameter guesses. The experimental verification was carried out using LEVM/LEVMW CNLS fitting program [1]. Fig. 3 demonstrates this problem.

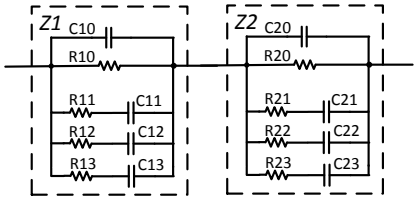


(a)

$$C_{\Sigma 1}(guesses1) = \sum_i C_{1i}$$

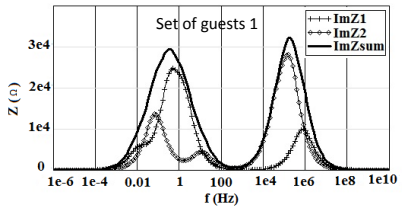


$$C_{\Sigma 2}(guesses1) = \sum_i C_{2i}$$

(b)

$$C_{\Sigma 1}(guesses2) = \sum_i C_{1i}$$

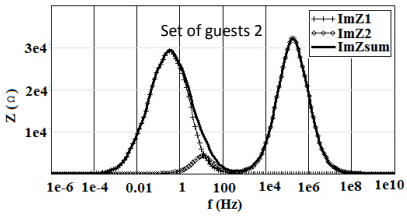


$$C_{\Sigma 2}(guesses2) = \sum_i C_{2i}$$

(c)

$$\mathrm{Im}\, Z_{sum}^{guesses1} = \mathrm{Im}\, Z_{sum}^{guesses2}$$

$$C_{\Sigma 1}(guesses1) \neq C_{\Sigma 1}(guesses2) \qquad C_{\Sigma 2}(guesses1) \neq C_{\Sigma 2}(guesses2)$$

Fig. 3. "Cross talking effect": different results for different guesses. (a) - electrical model; (b) and (c) – imaginary parts of impedance of the left and right parts of the model and their sum.

We used synthetic data and a simple case, where the characteristic time constants are clearly separated. In a real experiment, the situation is much more complicated.

Another method of parametric identification is building a parametric distribution function of relaxation times, the convolution of which generates a best possible fit to the experimental data. The distribution function can be composed of a series of peaks such as Gaussian, Lorentzian, hyperbolic secant, etc. The ISGP [2] is one of the programs that perform this task.

The impedance spectra of some electroceramics (such as barium titanate) are well described using a series of Gaussian peaks.

Gauss Impedance (GI) is presented as a convolution of the Gaussian ($G$) with the impedance kernel ($Kz$):

$$Z(\omega) = \int_0^\infty G(\tau) Kz(\omega, \tau)\, d\tau \tag{1}$$

$$G(\tau) = \frac{R_h}{\sigma\sqrt{2\pi}} \exp\left[ -\frac{\left(lg(\tau) - \lg(\tau_0)\right)^2}{2\sigma^2} \right] \tag{2}$$

where: $R_h$ – height, $\sigma$ – standard deviation, $\tau_0$ – characteristic time constant, $\tau$ – range of existence in the time domain, $\omega$ - angular frequency. Additionally

$$Kz(\omega, \tau) = \frac{1}{1 + j\omega\tau} \tag{3}$$

is the Debye kernel of impedance [1].

Various properties of Gauss Impedance were investigated. The GI is the generalization of Delta Function Impedance (DFI) – the convolution of the delta function with the Debye Kernel (3). The GI degenerates into DFI when the standard deviation approaches zero. A simple example of DFI is the impedance of a parallel lumped *RC*-circuit. The similarity between GI to DFI is demonstrated by the fact that GI has the same slope as DFI not far beyond characteristic frequency at any standard deviation. As will be seen later, this property of GI allows us to construct a 'true' asymptotic model.

Several other functions have been investigated. In this context, we shall discuss the functions that demonstrate a peak shape in the imaginary part of impedance, and have a peak in DFRT respectively. These functions are as follows [1]: ZARC, Cole-Cole, Lorentzian, hyperbolic secant, Warburg. These functions are used for fitting, but do not share the similarity to DFI that GI has. As a consequence, we do not have the ability to construct a true asymptotic model. They can only be marked as the 'observable' asymptotic model that may be a sufficient result in some cases. Another way to get a true asymptotic model is to utilize Gauss DFRT convoluted on a more complicated core (4).

$$Kz(\omega, \tau) = \frac{1}{\left[1 + (j\omega\tau)^\alpha\right]^\beta} \tag{4}$$

where $0 < \alpha < 1$ is a depression factor and $0 < \beta < 1$ is a non-symmetric parameter.

A set of individual impedance segments and sets of DFRT's parameters ($R_h$, $\sigma$, $\tau_0$ – for Gaussian type of DFRT) are found as a result of the above step of decomposition.

In some cases, it is difficult to gain physical interpretation of part of these parameters. We propose to use an asymptotic approach towards the construction of the electrical model, which is more familiar and informative to researchers.

### 3. ASYMPTOTIC MODEL INTERPRETATION

Now each of the impedances may be calculated from experimental DFRTs and can be treated individually. The aforementioned properties of GI allow us to perform asymptotic decomposition of the GI according to the model, Fig. 4:

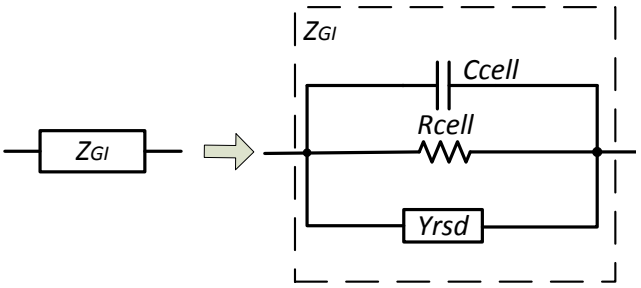


Fig. 4. The first step of asymptotic decomposition.

The model consists of the cell parameters and a residual admittance $Y_{rsd}$. The asymptotic values of the cell parameters $C_{cell}$ and $R_{cell}$ are:

$$C_{cell} = -\frac{1}{\omega \operatorname{Im} Z(\omega \to \infty)} \tag{5}$$

$$R_{cell} = \operatorname{Re} Z(\omega \to 0) \tag{6}$$

The accuracy of the asymptotic model depends on the distance of the frequencies chosen to determine the cell parameters from the characteristic frequency $f_0=1/2\pi\tau_0$. Taking frequencies six orders of magnitude larger and smaller than the characteristic frequency is sufficient for this calculation. In this case the relative errors are less than 0.01% in practical situations.

The residual admittance $Y_{rsd}$ (Fig. 4) represents a relaxation process in the cell, and is a measure of the distributed nature of the relevant process or structure. In a further step of asymptotic decomposition, the residual admittance $Y_{rsd}$ can be presented according to the flow diagram, Fig. 5.

The asymptotic values at low frequencies are characterized by a relaxation capacitance $C_{rlx}$:

$$C_{rlx} = \frac{\operatorname{Im} Y_{rsd}}{\omega(\omega \to 0)} \tag{7}$$

and at high frequencies by a relaxation resistance $R_{rlx}$:

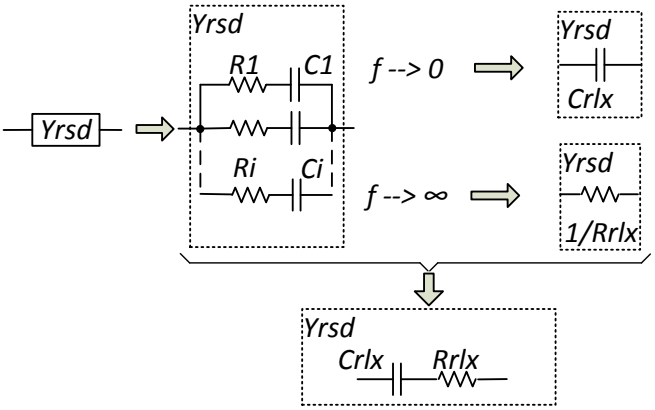


Fig. 5. Flow diagram for asymptotic decomposition of the residual admittance $Y_{rsd}$.

$$R_{rlx} = \frac{1}{\operatorname{Re} Y_{rsd}(\omega \to \infty)} \tag{8}$$

The final electrical model taking both steps of asymptotic decomposition into account is presented in Fig. 6.

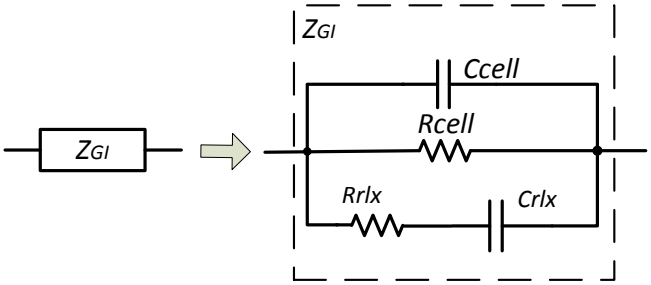


Fig. 6. Final model after two steps of asymptotic decomposition.

An unexpected result of the two-step decomposition of Gauss Impedance is that the time constants for cell parameters and relaxation parameters are equal:

$$C_{cell} \cdot R_{cell} = C_{rlx} \cdot R_{rlx} \tag{9}$$

Additionally, the cell and relaxation parameters are equal to the first segment of the ladder model, shown in Fig. 7. This condition is satisfied for infinite approximation only.

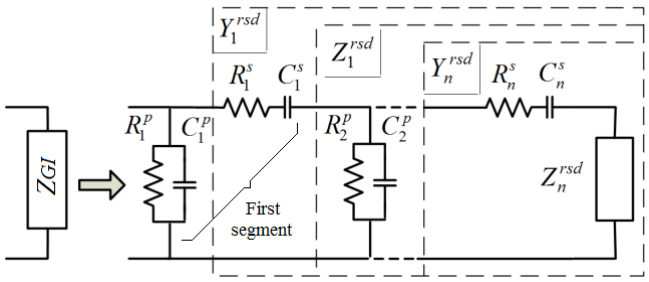


Fig. 7. Ladder representation of GI.

The experimental verification was carried out using LEVM/LEVMW CNLS fitting program [1]. We specified 18 free parameters and chose a data-proportional weighting

factor. Invariability of the time constants was confirmed for each fragment of the circuit. The corresponding equation (utilizing R and τ) has the following form:

$$Z = \frac{1}{\frac{1+j\omega\tau}{R_1^p} + \frac{1}{R_1^s + \frac{R_1^s}{1+j\omega\tau} + \frac{1}{\frac{1+j\omega\tau}{R_2^p} + \dots}}} \qquad (10)$$

Likewise this equation can be obtained using C and τ. The invariable nature of the time constant in (10) is emphasized. In this way, the number of free parameters is reduced by half plus one.

The relationship between Gauss DFRT and the corresponding asymptotic model has been established. The relations between normalized ($R_h$ = 1 Ω and $\tau_0$ = 1 s) cell capacitance $Cn_{cell}$ and the standard deviation of the Gaussian are summarized in Table 1.

Table 1. $Cn_{cell}$ vs. standard deviation $\sigma$ of the Gaussian

| $\sigma$ | 0.1 | 0.2 | 0.3 | 0.4 | 0.5 |
|---|---|---|---|---|---|
| $Cn_{cell}$ (F) | 0.973 | 0.899 | 0.787 | 0.654 | 0.515 |
| $\sigma$ | 0.6 | 0.7 | 0.8 | 0.9 | 1 |
| $Cn_{cell}$ (F) | 0.385 | 0.273 | 0.183 | 0.117 | 0.071 |

An attempt to find an analytical relation between parameters in Table 1 has led to an interesting result. It turns out that the relationship is also well described by the Gaussian:

$$Cn_{cell}(\sigma) = \frac{H}{\Sigma \cdot \sqrt{2\pi}} \exp\left[ -\frac{(\sigma - \sigma_0)^2}{2 \cdot \Sigma^2} \right] \qquad (11)$$

Here free parameters were found by fitting: $H$=1.088608, Σ=0.434296 and $\sigma_0$=0.

The fitting result reveals, using Eq. (11), a relative error of less than $10^{-3}$ % for each point of fitting. Expression (11) allows us to find the value of the $Cn_{cell}$ directly from $\sigma$ without calculation of the asymptotic capacitance. Actual values may be obtained from the normalized parameters utilizing experimental values $\tau_{0exp}$ and $R_{hexp}$ according to the equation:

$$C_{cell} = \frac{\tau_{0exp}}{R_{hexp}} Cn_{cell} \qquad (12)$$

We were unable to find an analytic expression relating between the relaxation parameters and the standard deviation. We used spline interpolation of given table values calculated beforehand by asymptotic decomposition.

Actual values of the relaxation parameters may be obtained from the normalized one using a formula similar to (12) and (9).

## 4. EXPERIMENTAL

The impedance measurements were performed on disks of dense ceramic samples of barium titanate with approximate dimensions of 9.8 mm diameter and 1.2 mm width. The electrodes were painted using a commercial Pt paste. The measurements were performed in the temperature range 200 ºC < $T$< 475 ºC, and the frequency range 10 mHz < $f$ < 30 MHz using Precision Impedance Analyser (Agilent 4294A) for high frequency range and Lock-in Amplifier (SR-830, Stanford Research) for low frequency range.

A representative example of the Nyquist plot for a sample at T=325 ºC and its fitting is shown in Fig. 8.

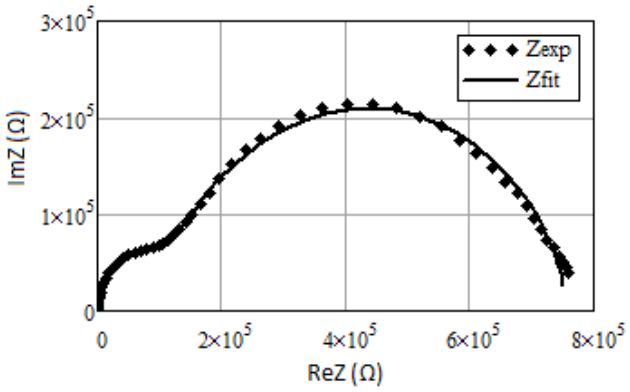


Fig. 8. Nyquist plot of experimental and fitted data for sample at T=325 ºC.

Fitting was carried out using a Gauss distribution function of relaxation times according to (2) and the convolution (1). The fitting program was created in LabVIEW environment using the Global Optimization function based on a differential evolution method.

Optimal fitting was obtained using two Gauss DFRTs convoluted into impedance using core (3), Fig 9.

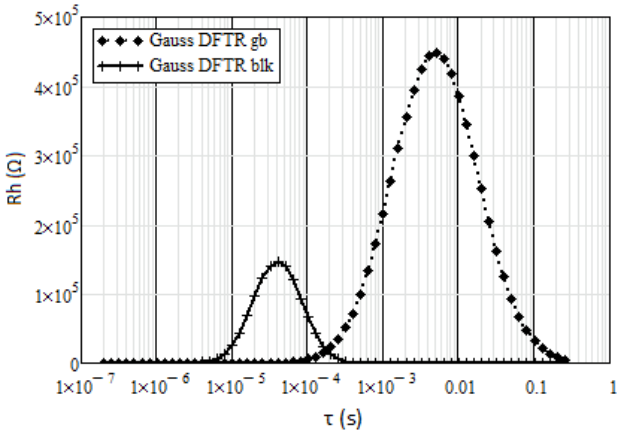


Fig. 9. Set of Gauss DFRTs (fitted result) at T=325 ºC.

The right Gaussian (low frequency range) is associated with grain boundaries, the left one (high frequency range) – with the bulk.

The cell and relaxation parameters were found using fitting results over the temperature range.

The temperature behavior of the cell parameters is shown in Fig. 10 and 11.

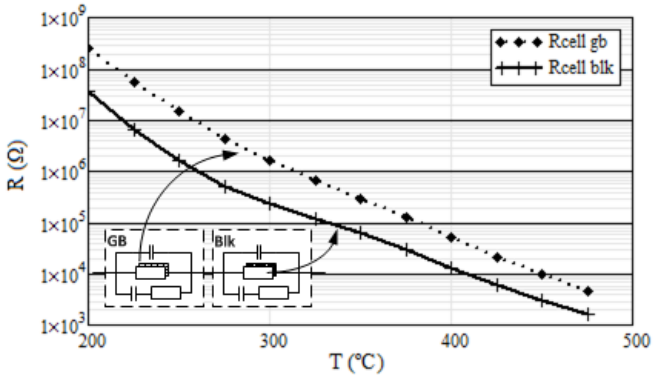


Fig. 10. The temperature behavior of $R_{cell}$ for the grain boundaries and the bulk.

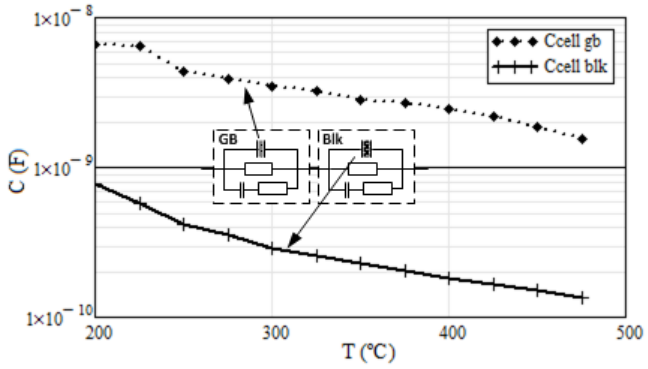


Fig. 11. The temperature behavior of $C_{cell}$ for the grain boundaries and the bulk.

The temperature dependence of the relaxation parameters is presented in Fig. 12 and 13.

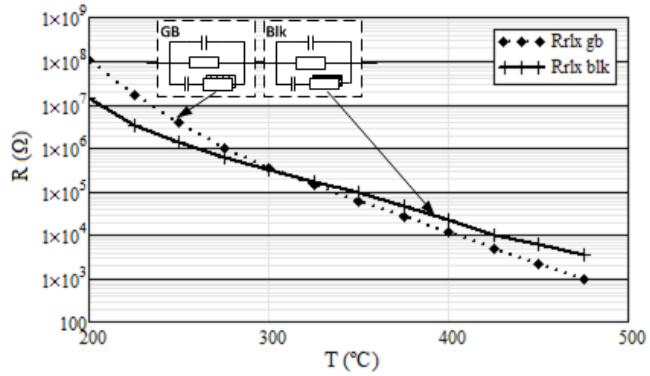


Fig. 12. The temperature behavior of $R_{rlx}$ for the grain boundaries and the bulk.

Experimental results demonstrate the possibility of performing more detailed studies into the behaviour of electroceramic objects.

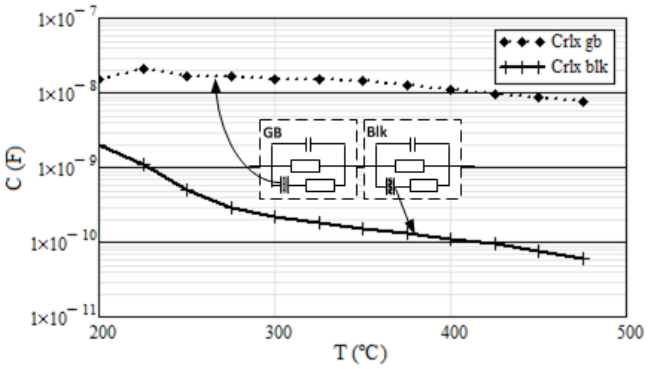


Fig. 13. The temperature behavior of $C_{rlx}$ for the grain boundaries and the bulk.

For example, one can separately estimate the activation energy of both the cell and relaxation processes. Arrhenius plots were built based on the data presented in Fig. 10 and 12. The calculated activation energy is specified in Table 2.

Table 2. Activation energy.

| Place | Grain Boundaries | Bulk |
|---|---|---|
| Cell | 1.18 eV | 1.06 eV |
| Relaxation | 1.24 eV | 0.89 eV |

This result is consistent with [1]. It is also possible to estimate the density of the relaxation centers (or the dielectric constant) for both the grain boundaries and the bulk as a function of temperature.

## 5. DISCUSSION

Each process or structure may be presented using two unambiguously interrelated forms: impedance and the distribution function of time constants. Parametric properties of these two representations are used to investigate electrochemical behavior. The unifying element of these two concepts is an identical impedance kernel.

Construction of the DFRT as the first step in our treatment allows the derivation of an unambiguous parametric model through fitting of experimental data. Additionally, it enables separation of the complete distribution function of relaxation times into independent parametric segments that may be treated separately.

The output parameters of DFRT are often difficult to link with electrochemical properties or behavior of the object under examination. Electrical models or equivalent schemes can help to solve this problem. The second stage – the transformation of each DFRT segment into corresponding impedance – bridges between the obtained parameters of the DFRT and the parameters of a relevant electrical model. In our case, this role is played by the asymptotic model.

It should be noted that the parameters of the asymptotic model (Fig. 6) will differ significantly from the parameters of the approximation model of the same topology. In other words, the asymptotic model cannot be obtained directly by

least squares fitting of the appropriate impedance, irrespective of fitting techniques.

The cell capacitance $C_{cell}$ demonstrates an instant response to electrical stimulation, and the resistance of the cell $R_{cell}$ characterizes the direct current conductivity.

The relaxation capacitance $C_{rlx}$ relates to the density of relaxation centers in specific regions of the sample, while $R_{rlx}$ describes the characteristic time constant.

It should be emphasized that the convolution of DFRT into impedance (direct problem) overcomes the drawback of the deconvolution (inverse or ill posed problem). This conversion is carried out unambiguously and without significant errors. Moreover, in some cases it is possible to establish a direct relation between the DFRT and an electrical model in advance. Here we utilized Gauss Impedance, which does not exist in analytical form – the GI is a result of convolution of the Gaussian with the impedance core. The asymptotic decomposition of GI looks like a series expansion. The first two terms of this series have a definite physical meaning. It is not necessary to know the form of the residual admittance $Y_{rsd}$ (as it appears in the model in Fig. 4) in order to determine the four basic parameters according to the model in Fig. 6.

If the object of a study imposes restrictions of the type of function of the residual admittance, then the parameters of the asymptotic model may serve as guesses for further investigation. In some cases, the residual admittance can be well described by the convolution of a Gaussian distribution of relaxation times (by changing the parameter in (2) from $R_h$ to $C_h$) with the admittance kernel:

$$Ky(\omega,\tau) = \frac{j\omega}{1+ j\omega\tau} \tag{13}$$

Statistical distribution of relaxation centers takes on a physical meaning in this case. This allows the electrical properties of the interface states such as the density of the traps at different electrode-electrolyte interfaces to be studied.

The resulting models may be transformed into other configurations without significant errors according to the vision of the researcher.

The experimental results demonstrate the possibility of performing more detailed studies into the behavior of electroceramic objects. For example, one can separately estimate the activation energy of both the cell and relaxation processes. It is also possible to estimate the density of the relaxation centers (or the dielectric constant) for both the grain boundaries and the bulk.

## 6. CONCLUSIONS

The direct fitting of full impedance spectra by a detailed equivalent circuit is challenging due to ambiguity. An interpretation technique of impedance spectra is proposed, which extends the possibilities of impedance spectroscopy analysis.

Our method is based on decomposition of experimental spectra into independent impedance segments. We have demonstrated how to convert the parameters of analytical DFRT into a more familiar equivalent circuit using an asymptotic approach. Mostly monotonic behaviour of the asymptotic parameters versus temperature confirms the validity of this approach.

The essential features of the Gauss Impedance are revealed during the creation of the asymptotic model: (i) – similarity between GI and DFI; (ii) – invariable time constant, see (9); (iii) – asymptotic model equal to the first segment of the infinite ladder circuit, Fig. 7 and (iv) – Gaussian's relation between cell capacitance and standard deviation, see (11). These properties require further study in order to reach a thorough understanding.

## ACKNOWLEDGMENTS

The author wishes to thank the Center for Absorption in Science and the Ministry of Immigrant Absorption for their support.

## REFERENCES

[1] E. Barsoukov, R. Macdonald (Eds.), *Impedance Spectroscopy, Theory, Experiment, and Applications*, 2nd Ed., John Wiley & Sons. Inc., New Jersey, 2005.

[2] Hershkovitz, S., Baltianski, S., Tsur, Y. "Electrochemical Impedance Analysis of SOFC Cathode Reaction Using Evolutionary Programming", *Fuel Cells*, vol. 12, pp. 77-85, February 2012.